



## REVIEW ARTICLE

# Neuroimaging features of FOXR2-activated CNS neuroblastoma: A case series and systematic review

Kenichiro Shimazaki<sup>1</sup> | Ryo Kurokawa<sup>1</sup>  | Andrea Franson<sup>2</sup>  |  
 Mariko Kurokawa<sup>1</sup>  | Akira Baba<sup>1</sup>  | Laura Bou-Maroun<sup>2</sup> | John Kim<sup>1</sup> |  
 Toshio Moritani<sup>1</sup>

<sup>1</sup>Division of Neuroradiology, Department of Radiology, University of Michigan, Ann Arbor, Michigan, USA

<sup>2</sup>Division of Pediatric Hematology/Oncology, Department of Pediatrics, Ann Arbor, Michigan, USA

## Correspondence

Ryo Kurokawa, Division of Neuroradiology, Department of Radiology, University of Michigan, 1500 E Medical Center Dr, UH B2, Ann Arbor, MI 48109, USA.  
 Email: [kuroro63@gmail.com](mailto:kuroro63@gmail.com)

## Funding information

None

## Abstract

**Background and Purpose:** CNS neuroblastoma, FOXR2-activated (CNS NB-FOXR2) is a newly recognized tumor type in the 2021 World Health Organization classification of central nervous system (CNS) tumors. We aimed to investigate the clinical and neuroimaging findings of CNS NB-FOXR2 and systematically review previous publications and three new cases.

**Methods:** We searched PubMed, SCOPUS, and Embase databases for patients with pathologically proven CNS NB-FOXR2 with sufficient information for preoperative CT and MRI findings. Two board-certified radiologists reviewed the studies and imaging data.

**Results:** Thirty-one patients from six previous publications and 3 patients from our hospital comprised the study population (median age, 4.2 [range: 1.4–16] years; 19 girls). Clinically, CNS NB-FOXR2 mainly affected children between 2 and 6 years (24/34, 67.6%). Nausea/vomiting and seizures were reported as the main presenting symptoms (100% in total). The tumors frequently showed hyperdensity compared to the cortex on nonenhanced CT (4/5, 80%) with calcification along the inner rim of the tumor (4/5, 80%). More than half of patients showed susceptibility artifacts indicating intratumoral hemorrhage and/or calcification (15/28, 53.6%) on T2\*- and/or susceptibility-weighted imaging. Elevated relative cerebral blood volume and flow and percentile signal recovery were observed in one case with dynamic susceptibility contrast MRI.

**Conclusions:** Characteristic imaging features including hyperdense attenuation of the solid components and calcification along the inner rim on CT and susceptibility-weighted imaging may assist with preoperative diagnosis of CNS NB-FOXR2 in pediatric patients.

## KEYWORDS

computed tomography, FOXR2, magnetic resonance imaging, neuroblastoma, systematic review

## INTRODUCTION

CNS neuroblastoma, FOXR2-activated (CNS NB-FOXR2) is a newly recognized tumor type in the World Health Organization (WHO) classification of central nervous system (CNS) tumors in 2021.<sup>1</sup> This tumor

is an embryonal neoplasm exhibiting varying degrees of neuroblastic and/or neuronal differentiation and is characterized by activation of the transcription factor FOXR2 by structural rearrangements.<sup>2</sup> CNS NB-FOXR2 was formerly recognized as part of primitive neuroectodermal tumors of the CNS (CNS-PNETs), indistinguishable from other

This is an open access article under the terms of the [Creative Commons Attribution-NonCommercial](https://creativecommons.org/licenses/by-nc/4.0/) License, which permits use, distribution and reproduction in any medium, provided the original work is properly cited and is not used for commercial purposes.

© 2023 The Authors. *Journal of Neuroimaging* published by Wiley Periodicals LLC on behalf of American Society of Neuroimaging.



embryonal tumors. However, CNS NB-FOXR2 is now recognized as one of the “other (ie, other than medulloblastoma) CNS embryonal tumors” category in the WHO classification in 2021, as with atypical teratoid/rhabdoid tumors; cribriform neuroepithelial tumors (provisional type); embryonal tumors with multilayered rosettes; CNS tumors with BCOR internal tandem duplication; and CNS embryonal tumors.<sup>1</sup>

CNS NB-FOXR2 most commonly presents as a mass in the cerebral hemisphere with a peak incidence at the age of 5 years and a slightly female preponderance.<sup>2,3</sup> Patients often present with signs of supratentorial masses including headache, vomiting, seizures, and focal neurological deficits.<sup>4</sup> The mainstay of the treatment is maximal surgical resection followed by chemotherapy and/or radiation.<sup>5</sup> The prognosis of CNS NB-FOXR2 is better than that of other embryonal tumors, with 5-year progression-free survival (PFS) and 5-year overall survival (OS) of 63% and 85%, respectively.<sup>6-8</sup> Additionally, based on retrospective review, CNS NB-FOXR2 tumors are seemingly more chemo-sensitive than other tumors previously under the larger “PNET” categorization.<sup>6</sup>

While the understanding of the pathology is increasing and clinical features have been gradually recognized, knowledge of radiological features of CNS NB-FOXR2 has been limited to mainly case-based reports. Given the rarity of the tumor type, no systematic review has been performed to date, therefore its characteristics are poorly understood, especially on CT.

The purpose of this study was to perform a systematic review of clinical and neuroimaging characteristics of CNS NB-FOXR2.

## METHODS

### Study selection

We searched PubMed, SCOPUS, and Embase databases using the following search terms on December 2, 2022, with no date limits:

- (neuroblastoma) AND (FOXR2) AND ((radiology) OR (neuroradiology) OR (imaging) OR (computed tomography) OR (CT) OR (magnetic resonance) OR (MRI))

Publications were considered eligible if they included all of the following criteria:

- Sufficient information for CT or MRI imaging findings of CNS NB-FOXR2 was available;
- The tumors were pathologically proven as CNS NB-FOXR2;
- Each patient’s demographic data were available.

Exclusion criteria were as follows:

- Duplicate cases;
- Not written in English;
- Insufficient information for MRI and CT;
- The content was irrelevant to CNS NB-FOXR2;
- Studies published as abstracts only (eg, conference proceedings).

We also obtained our institutional review board exemption for the inclusion of three cases with pathologically proven CNS NB-FOXR2 with preoperative CT and MR images from our hospital. Data were acquired in compliance with all applicable Health Insurance Portability and Accountability Act regulations.

This study was performed according to the Preferred Reporting Items for Systematic Reviews and Meta-Analyses (PRISMA) 2020 statement.<sup>9</sup>

### Data analyses

Two board-certified radiologists reviewed all studies and CT and MR images of the eligible examinations. When discrepancies arose between the two reviewers, the final decision was made after discussion.

### Collected data

The following data were collected:

#### Demographics

- Patient age
- Sex

#### Clinical

- Presenting complaint
- Recurrence after treatment (presence or absence)
- Survival outcomes (survived or dead)
- Follow-up duration (month since diagnosis)

#### Imaging

- Tumor size, laterality, and location
- Involvement of ventricular system
- Involvement of cortex
- Involvement of deep white matter
- Presence or absence of calvarial remodeling
- The degree of peritumoral edema
- The degree of hydrocephalus
- Percentage of enhancement of solid part
- Strength of enhancement
- Predominant signal intensity on T2-weighted imaging (WI) or fluid-attenuated inversion recovery images
- Presence or absence of hyperintensity on DWI
- Mean apparent diffusion coefficient (ADC)
- Presence or absence of nonsolid component
- Predominant signal density on CT
- Presence or absence of calcification of internal rim
- The cause of susceptibility artifact on T2WI and/or susceptibility-weighted imaging (SWI)
- Relative cerebral blood volume (rCBV) and flow (rCBF) and percentage signal recovery (PSR) on diffusion susceptibility contrast perfusion MRI

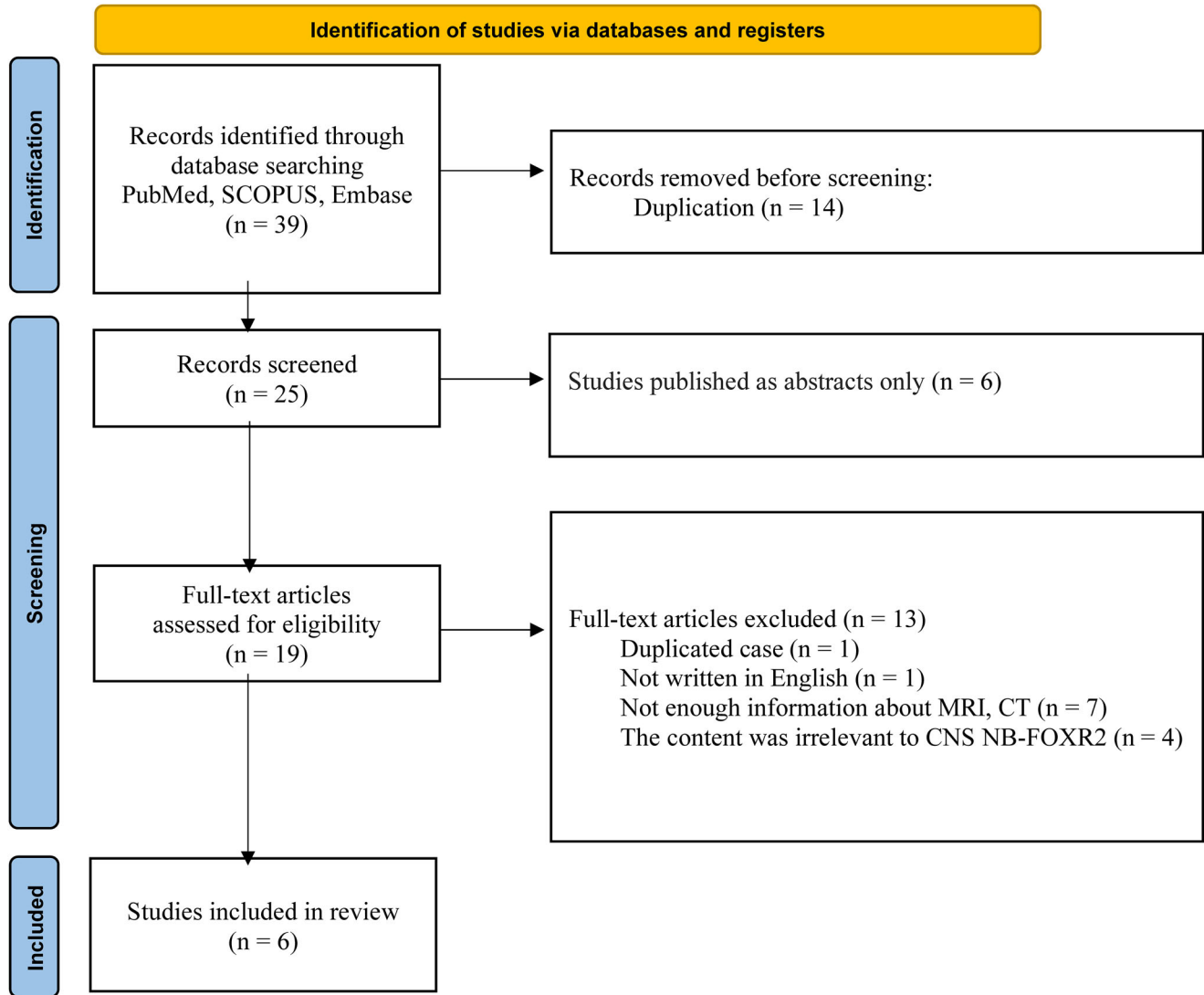


**FIGURE 1** Flow diagram of study identification. SCOPUS is Elsevier's abstract and citation database. *n*, number of records.

The following formula was used to calculate PSR:<sup>10</sup>

$$\text{PSR} = 100\% \times ((S1 - S_{\min}) / ([S0 - S_{\min}]),$$

where  $S0$  is the baseline signal intensity averaged over the first 10 timepoints,  $S1$  is the tail averaged over the last 10 timepoints, and  $S_{\min}$  is the minimum  $T2^*$ -weighted signal intensity in the dynamic series. To calculate the PSR within the slice depicting the largest areas of the tumors, a circular region of interest (30–40 mm<sup>2</sup>) was placed within the solid components of the tumors.

### Risk of bias assessment

We employed a tool to evaluate the methodological quality of case reports and case series proposed by Murad et al.<sup>11</sup> This tool comprises

eight signaling questions in four domains—selection, ascertainment, causality, and reporting—and has been used in various previous case-based systematic reviews including our previous studies.<sup>12–17</sup>

## RESULTS

### Study selection

A database search using PubMed, SCOPUS, and Embase identified 39 abstracts. We screened these results according to the PRISMA 2020 guideline and narrowed them down to potentially eligible studies by removing duplicates, and irrelevant studies by title and abstract screening. After excluding 33 studies based on the exclusion criteria, six studies with 31 patients with CNS NB-FOXR2 satisfied the criteria for the systematic review.<sup>3,18–22</sup> Other than 25 case series by Tietze

**TABLE 1** Patient data in our hospital.

Patients	1	2	3
Age at diagnosis	6.7 years	1.6 years	2.6 years
Sex	Girl	Girl	Boy
Onset symptom	1-week history of nausea/vomiting	1.5-month history of seizures	New-onset right-sided seizures
Treatment	Surgery, chemotherapy, radiation, stem cell transplantation	Surgery	Surgery
Recurrence	No	No	No
Patient status	Survive	Survive	Survive
Follow up duration (month)	7	66	1
Maximum tumor diameter	89 mm	49 mm	37 mm
Laterality	Left	Left	Left
Tumor location	parietal, occipital, basal ganglia, thalamus, deep white matter	frontal	frontal, basal ganglia, deep white matter
Ventricular system involvement	Yes	No	Yes
Cortical involvement	Yes	Yes	No
Calvarial remodeling	Yes	Yes	No
Peritumoral edema	Little	None	None
Hydrocephalus	Moderate	None	None
Percent enhancement of solid part	75%-100%	50%-75%	50%-75%
Strength of enhancement	Strong	Intermediate	Intermediate
Predominant T2-weighted imaging/ fluid-attenuated inversion recovery signal intensity <sup>a</sup>	Hyperintense	Hyperintense	Hyperintense
Diffusion-weighted imaging hyperintensity	Yes	Yes	Yes
Mean apparent diffusion coefficient (10 <sup>-6</sup> mm <sup>2</sup> /second)	670	701	658
Nonsolid component	Yes	Yes	Yes
Predominant CT attenuation <sup>a</sup>	Isodense	Hyperdense	Hyperdense
Hemorrhage	Yes	No	No
Calcification along the inner rim	Yes	Yes	No

<sup>a</sup>Compared to the cortex.

et al.,<sup>22</sup> which focused on MR imaging features, these studies were case-based reports.<sup>3,18-21</sup> The study selection process is summarized in the flow diagram in Figure 1. One review article was excluded since the duplicated case (patient #2 in our hospital) with different images was included.<sup>23</sup> The studies in this systematic review were conducted between 2018 and 2022. Additionally, we included three patients with CNS NB-FOXR2 from our hospital (Table 1), resulting in a final study cohort of 34 patients.

### Risk of bias assessment

As we extracted data from case-based studies, in which the selection method was rarely mentioned, selection bias may have been introduced. Tumor size was available in 15 cases (44.1 %). Treatment strategy and survival outcomes were reported for 6 (17.6 %) and 7 (20.6 %) patients, respectively. Patients' follow-up duration of the patients varied from 1 month to 11.7 years. Since we evaluated the cases with

information on preoperative CT and/or MR images, our investigation on imaging findings can be replicated by other investigators.

### Demographic and clinical data

The demographic and clinical data of 34 patients are summarized in Table 2. The median age was 4.2 years (range: 1.4-16 years). Patients 2-6 years of age (23/34, 67.6%) were mainly affected; however, 5 of 34 patients (14.7%) were  $\geq 10$  years old. Girls (19/34, 55.9%) were more frequently affected than boys.

Among the patients with known presenting history, nausea, vomiting, and seizure were typically observed at presentation.

### Neuroimaging data

The neuroimaging findings are summarized in Table 3.

**TABLE 2** Demographic and clinical information of 34 patients with CNS neuroblastoma, FOXR2-activated

Demographic	
Median age (years [range]) (n = 34)	4.2 [1.4-16]
Sex	Boys = 15, Girls = 19
Clinical	
Nausea/vomiting	3/6 (50.0%)
Seizures	3/6 (50.0%)
Recurrence after gross total resection	0/5
Follow up duration (months [range]) (n = 27)	18.8 [1-139.8]
Survival status	6/7 (85.7%)

Abbreviation: n, number of patients.

All tumors were located in the supratentorial regions, with one tumor involving the brainstem and cerebellum simultaneously. Tumors showed hyperdensity (4.5, 80.0%) or isodensity (1/5, 20.0%) compared to the cortex on nonenhanced CT. Calcification along the inner rim of the tumor was observed in 4 of 5 (80.0%) patients with available CT images, including two of our patients. Susceptibility artifacts were caused by hemorrhage and/or calcification (15/28, 53.6%). Nonsolid components were observed in all but one case (33/34, 97.1%). Involvement of the cortex (29/34, 85.3%), deep white matter (33/34, 97.1%), and ventricular system (21/34, 61.8%) was frequently observed. Tumors usually showed low ADC (median mean ADC =  $659 \times 10^{-6}$  mm<sup>2</sup>/second; range: 488-1070  $\times 10^{-6}$  mm<sup>2</sup>/second; 24 patients). The whole tumor volume-of-interest-derived rCBV and rCBF of our patient #1 were 2.673 mL/100 g and 34.143 mL/100 g/minute, respectively, and PSR was 141.7%. CT and MR images of the 3 patients in our hospital are shown in Figures 2-4.

## DISCUSSION

In this systematic review, we summarized the clinical and neuroimaging findings of 34 patients with CNS NB-FOXR2 including 3 patients from our hospital. We discovered that hyperdense mass with calcification along the inner rim may be characteristic imaging features on nonenhanced CT. Susceptibility artifacts were found in more than half of patients, and phase images on SWI could differentiate hemorrhage and calcification as shown in the 2 patients from our hospital. We also reported dynamic susceptibility contrast (DSC)-MRI findings in one case, which have not been previously described in the literature.

CNS NB-FOXR2 is known for its complex interchromosomal and intrachromosomal rearrangements in the FOXR2 gene, producing a fusion between the entire FOXR2 gene and other genes.<sup>1,24,25</sup> Although the pathomechanism has not yet been fully elucidated, stabilization and amplification of MYCN induced by activated FOXR2 are thought to play a pivotal role in tumorigenesis of CNS NB-FOXR2.<sup>26</sup> Histologically, it is reported that CNS NB-FOXR2 is composed of sheets

**TABLE 3** Neuroradiological characteristics of 34 patients with CNS neuroblastoma, FOXR2-activated

Maximum tumor diameter (median mm [range])	59.5 [37-89] (4 patients)
Tumor volume (median mL [range])	155.6 [11.9-340.5] (11 patients)
Laterality	Right = 15/34, Left = 17/34, Right and middle = 2/34
Location	
Frontal lobe	23/34 (67.6%)
Parietal lobe	13/34 (38.2%)
Temporal lobe	14/34 (41.2%)
Occipital lobe	5/34 (14.7%)
Basal ganglia	13/34 (38.2%)
Thalamus	5/34 (14.7%)
Brainstem	1/34 (2.9%)
Cerebellum	1/34 (2.9%)
Ventricular system involvement	21/34 (61.8%)
Cortical involvement	29/34 (85.3%)
Deep white matter involvement	33/34 (97.1%)
Calvarial remodeling	16/34 (47.1%)
Peritumoral edema	Extensive = 1/34, Moderate = 4/34, Little = 21/34, None = 8/34
Hydrocephalus	Extensive = 4/34, Moderate = 12/34, Mild = 7/34, None = 11/34
Percent enhancement of solid part	100% = 1/34, 75%-100% = 18/34, 50%-75% = 5/34, 25%-50% = 5/34, <25% = 2/34, 0% = 3/34
Strength of enhancement	Strong = 7/34, Intermediate = 19/34, Weak = 5/34, None = 3/34
Predominant T2-weighted imaging/ fluid-attenuated inversion recovery signal intensity <sup>a</sup>	Hyperintense = 31/34, Hyperintense and Isointense = 3/34
Mean apparent diffusion coefficient (median $10^{-6}$ mm <sup>2</sup> /second [range])	659 [488-1070] (24 patients)
Nonsolid component	33/34 (97.1%)
Susceptibility caused by	Hemorrhage only = 5/28, calcification only = 4/28, hemorrhage and calcification = 5/28, hemorrhage or calcification = 1/28, none = 13/28
Predominant CT attenuation <sup>a</sup>	Hyperdense = 4/5 (80.0%), Isodense = 1/5 (20.0%)
Calcification along the inner rim	4/5 (80.0%)

<sup>a</sup>Compared to the cortex.

of uniform, round, and poorly differentiated cells with a high nuclear-to-cytoplasmic ratio often accompanied by necrosis with relatively high mitotic count.<sup>3,27</sup>

Compared to other embryonal tumors and pediatric-type high-grade diffuse gliomas, the survival outcome of CNS NB-FOXR2 is

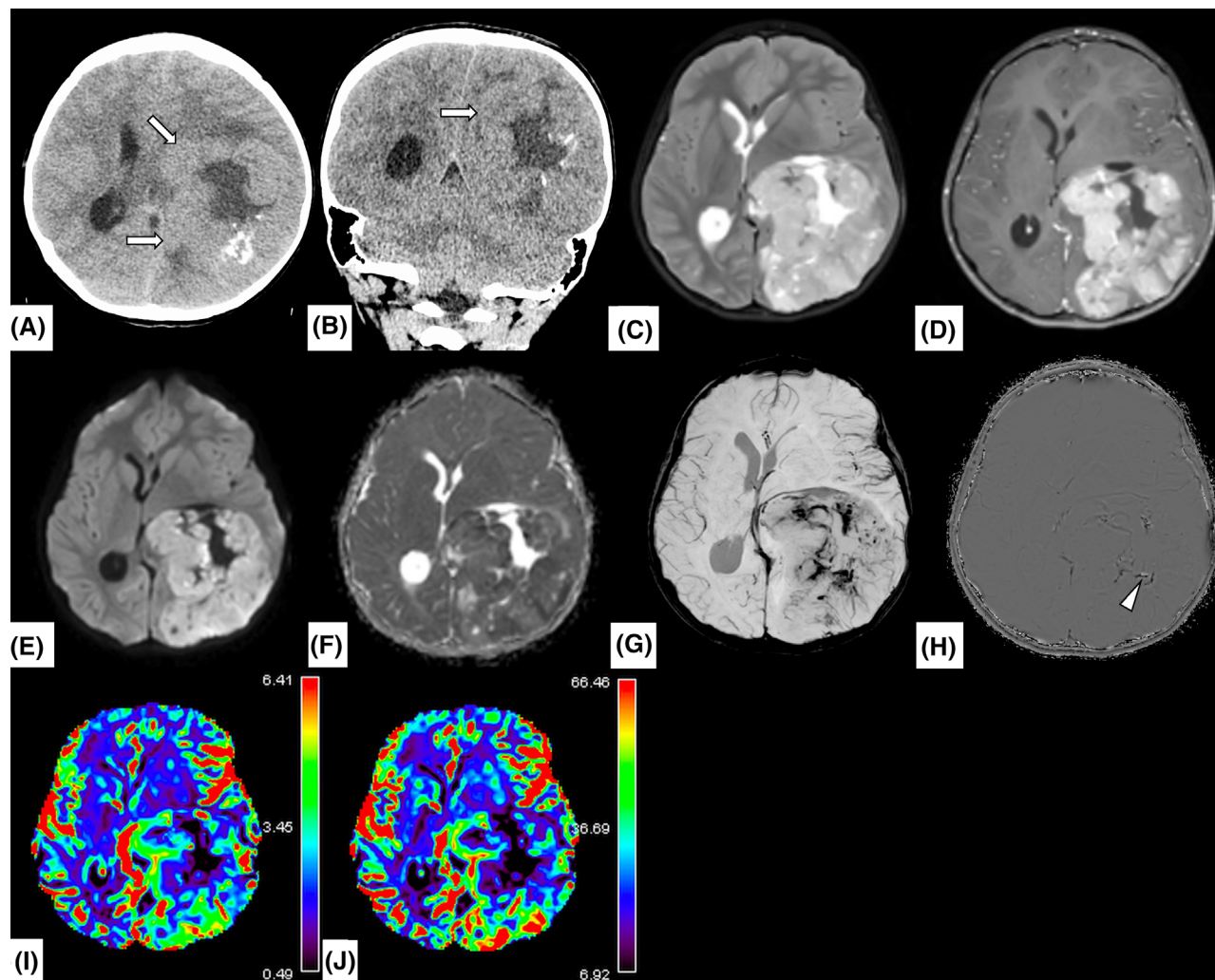


**FIGURE 2** CNS neuroblastoma, FOXR2-activated in a 6.7-year-old girl presenting with 1-week history of nausea/vomiting (patient #1; Ingenia, 1.5T; Philips Healthcare, Eindhoven). Axial (A, arrows) and coronal (B, arrow) nonenhanced CT show a large lobulated isodense mass in the left cerebral hemisphere with calcification along the inner rim of the tumor. Involvement of the cortex, deep white matter, basal ganglia, and lateral ventricle, moderate hydrocephalus, and nonsolid components are observed. MRI shows hyperintensity on T2-weighted image (C) with a strong enhancement in the solid components (D). The tumor shows hyperintensity on diffusion-weighted image (E) with a mean apparent diffusion coefficient of  $670 \times 10^{-6}$  mm<sup>2</sup>/second (F). Susceptibility-weighted image shows hypointensity areas with a blooming effect along the inner rim (G), and phase image shows both hyperintensity areas indicating calcification (H, arrowhead) and hypointensity areas indicating microhemorrhage. Diffusion susceptibility contrast MRI-derived relative cerebral value (I) and flow (J) are 2.673 mL/100 g and 34.143 mL/100 g/minute, respectively. Percentage signal recovery is calculated as 141.7%.

considered favorable. Katja et al. reported that 5-year PFS and 5-year OS of CNS NB-FOXR2 were 63% and 85%, respectively,<sup>6</sup> with 35 of 42 progression-free survivors after craniospinal irradiation and chemotherapy, which was comparable to the present study in patients where outcome data were known (5/6, 83.3%). Given that most favorable outcomes were achieved in patients who underwent some form of radiation therapy, Liu et al. recommend a risk-adapted cerebrospinal radiation-containing regimen for children  $\geq 3$  years and a cerebrospinal radiation-sparing regimen with focal radiation for children  $< 3$  years with localized disease.<sup>28</sup> Molecularly targeted therapy against FOXR2 may be effective, although historically, molecularly targeting a transcription factor directly is difficult and no small-molecule inhibitors of FOXR2 are available to date.

Clinically, CNS NB-FOXR2 mainly affected children between 2 and 6 years (67.6%) with a slight female predominance (55.9%). Nausea/vomiting and seizures are the main presenting symptoms (100% in total). Radiologically, CNS NB-FOXR2 were most often located in the frontal lobe (23/34, 67.6%) with frequent involvement of the cortex (29/34, 85.3%), deep white matter (33/34, 97.1%), and ventricular system (21/34, 61.8%). Tietze et al. reported that supratentorial location, often large size, multilobulated tumor shape, little-or-no peritumoral edema, presence of nonsolid components,<sup>22</sup> T2WI hyperintensity compared to the cortex, low ADC values, and susceptibility artifact on T2- or susceptibility-weighted images were frequently found, and these imaging features were also verified in this systematic review. We also identified that on nonenhanced CT, solid components of

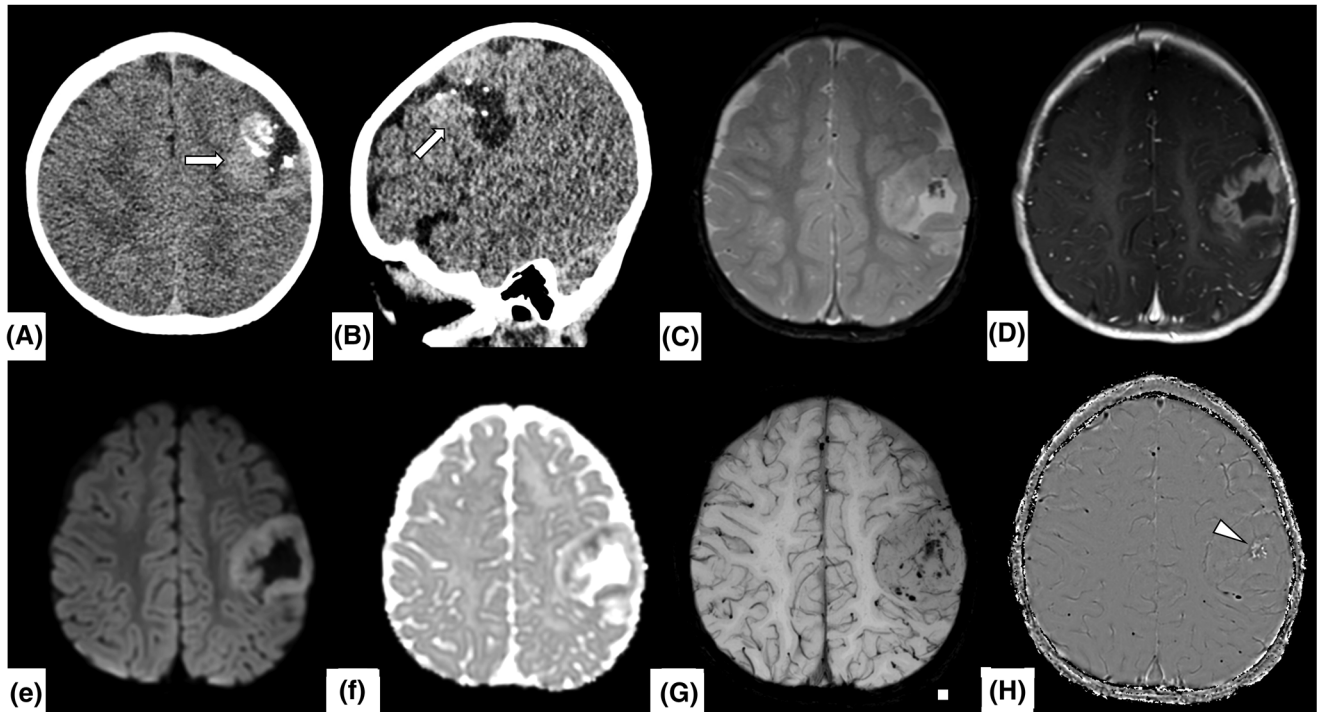


**FIGURE 3** CNS neuroblastoma, FOXR2-activated in a 1.6-year-old girl presenting with 1.5-month history of seizures (patient #2; Ingenia, 3T; Philips Healthcare, Eindhoven). Axial (A, arrows) and coronal (B, arrow) nonenhanced CT show a large lobulated hyperdense mass in the left frontal lobe with nonsolid components and calcification along the inner rim of the tumor. MRI shows hyperintensity on T2-weighted image (C) with an intermediate enhancement in the solid components (D). The tumor shows hyperintensity on diffusion-weighted image (E) with a mean apparent diffusion coefficient of  $701 \times 10^{-6}$  mm<sup>2</sup>/second (F). Susceptibility-weighted image shows hypointensity areas with a blooming effect along the inner rim (G), and phase image shows both hyperintensity areas indicating calcification (H, arrowhead).

CNS NB-FOXR2 appeared hyperdense (4/5, 80%) or isodense (1/5, 20%) relative to the cortex with characteristic calcification along the inner rim (4/5, 80%). The preferred tumor location may differentiate CNS NB-FOXR2 from medulloblastoma or diffuse midline glioma, H3K27-altered; the latter two are more common in the posterior fossa and the middle regions, respectively.<sup>29,30</sup> Age at presentation is different from that of infant-type hemispheric glioma (median: 2.8 months [range: 0-12 months] vs. 4.2 years [1.4-16 years] in CNS NB-FOXR2).<sup>1</sup> Furthermore, intratumoral calcification has been shown to be rare in diffuse hemispheric glioma, H3G34-mutant, atypical teratoid/rhabdoid tumors, or diffuse pediatric-type high-grade glioma, H3-wildtype, and isocitrate dehydrogenase-wildtype.<sup>17,31,32</sup> Hyperdensity on CT might have represented high tumor cellularity, and the inner rim calcification might be dystrophic along the necrotic areas induced by high mitotic activity. More than half of patients showed susceptibility artifacts within the tumors, although the breakdown of the used sequence for evaluation of susceptibility artifacts (ie, T2WI or SWI) was unknown. Given that SWI is more sensitive to susceptibility artifacts compared with T2WI,<sup>33</sup> the incidence of intratumoral hemorrhage or calcification could have been even higher if SWI was performed in all cases. Phase images on SWI could validate corresponding calcification as shown in Patients #1 and #2 from our hospital. The tumor in Patient #1 also displayed elevated rCBV, rCBF, and PSR on DSC-MRI, and to our knowledge, this is the first case

with DSC-MRI findings. Elevated rCBV and rCBF are nonspecific findings of hypervascularized tumors; however, a very high PSR has been reported to be more suggestive of lymphoma than glioblastoma in adult patients,<sup>10,34</sup> and therefore, it may be more suggestive of CNS NB-FOXR2 than other types of tumors, such as pediatric-type diffuse gliomas.

There were some limitations to this study. First, due to the rarity and recent recognition of the tumor type, the number of included patients was limited (34 patients). Second, most of the collected studies did not provide inclusion criteria because of the case-based nature. Third, many publications did not describe all the factors that we collected, due to the heterogeneity of the studies. For future directions, it would be helpful to accumulate knowledge of nuclear imaging findings including PET and contrast-enhanced perfusion MRI findings, which have not yet been established, for further understanding of CNS NB-FOXR2.

Based on the systematic review of the 34 cases of clinical and imaging findings of CNS NB-FOXR2, we came to a conclusion that hyperdense attenuation of the solid components and calcification along the inner rim may help the pretreatment diagnosis of CNS NB-FOXR2 on nonenhanced CT. Phase imaging on SWI could detect the corresponding calcification. In addition, high rCBV, rCBF, and PSR on DSC-MRI may also be characteristic for this recently recognized tumor type.

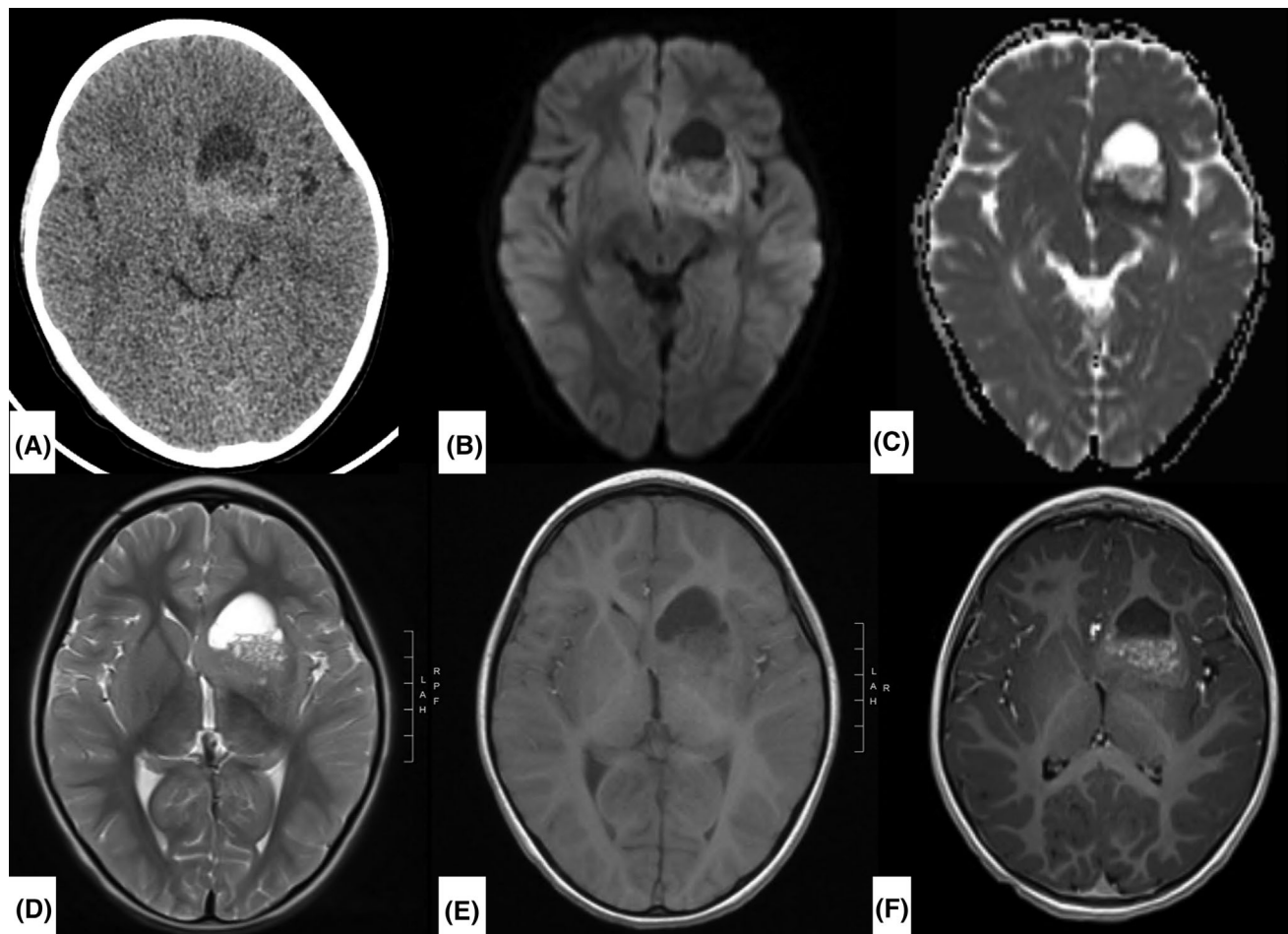


**FIGURE 4** CNS neuroblastoma, FOXR2-activated in a 2.6-year-old boy presenting with new-onset right-sided seizures (patient #3). Axial nonenhanced CT shows a hyperdense mass with nonsolid components centered in the left basal ganglia (A). Involvement of deep white matter and lateral ventricle is observed. The tumor shows hyperintensity on diffusion-weighted image (B) and T2-weighted image (D) and hyper-to-isointensity on T1-weighted image (E) with intermediate enhancement (F). Mean apparent diffusion coefficient is  $658 \times 10^{-6} \text{ mm}^2/\text{second}$  (C).

#### ACKNOWLEDGMENTS

We would like to thank Editage (<http://www.editage.com>) for editing and reviewing this manuscript for the English language.

#### CONFLICT OF INTEREST STATEMENT

The authors declare no conflicts of interest.

#### ORCID

Ryo Kurokawa <https://orcid.org/0000-0002-1186-8900>

Andrea Franson <https://orcid.org/0000-0002-5361-7683>

Mariko Kurokawa <https://orcid.org/0000-0002-3907-9188>

Akira Baba <https://orcid.org/0000-0001-6913-5307>

#### REFERENCES

- Louis DN, Perry A, Wesseling P, et al. The 2021 WHO classification of tumors of the central nervous system: a summary. *Neuro Oncol.* 2021;23:1231-51.
- Sturm D, Orr BA, Toprak UH, et al. New brain tumor entities emerge from molecular classification of CNS-PNETs. *Cell.* 2016;164:1060-72.
- Holsten T, Lubieniecki F, Spohn M, et al. Detailed clinical and histopathological description of 8 cases of molecularly defined CNS neuroblastomas. *J Neuropathol Exp Neurol.* 2021;80:52-9.
- Bianchi F, Tamburrini G, Gessi M, et al. Central nervous system (CNS) neuroblastoma. A case-based update. *Childs Nerv Syst.* 2018;34:817-23.
- PDQ Pediatric Treatment Editorial Board. Childhood medulloblastoma and Other Central Nervous System Embryonal Tumors Treatment (PDQ®): patient version. In: PDQ Cancer Information Summaries. National Cancer Institute (US); 2020.
- Von Hoff K, Haberler C, Schmitt-Hoffner F, et al. Therapeutic implications of improved molecular diagnostics for rare CNS embryonal tumor entities: results of an international, retrospective study. *Neuro Oncol.* 2021;23:1597-611.
- Mynarek M, Von Hoff K, Pietsch T, et al. Nonmetastatic medulloblastoma of early childhood: results from the prospective clinical trial HIT-2000 and an extended validation cohort. *J Clin Oncol.* 2020;38:2028-40.
- Upadhyaya SA, Robinson GW, Onar-Thomas A, et al. Relevance of molecular groups in children with newly diagnosed atypical teratoid rhabdoid tumor: results from prospective St. Jude multi-institutional trials. *Clin Cancer Res.* 2021;27:2879-89.





9. Page MJ, McKenzie JE, Bossuyt PM, et al. The PRISMA 2020 statement: an updated guideline for reporting systematic reviews. *BMJ*. 2021;372:n71.
10. Lee MD, Baird GL, Bell LC, et al. Utility of percentage signal recovery and baseline signal in DSC-MRI optimized for relative CBV measurement for differentiating glioblastoma, lymphoma, metastasis, and meningioma. *AJNR Am J Neuroradiol*. 2019;40:1445-50.
11. Murad MH, Sultan S, Haffar S, et al. Methodological quality and synthesis of case series and case reports. *BMJ Evid Based Med*. 2018;23:60-3.
12. Kurokawa M, Kurokawa R, Capizzano AA, et al. Neuroradiological features of the polymorphous low-grade neuroepithelial tumor of the young: five new cases with a systematic review of the literature. *Neuroradiology*. 2022;64:1255-64.
13. Baba A, Kurokawa R, Kurokawa M, et al. Imaging features of laryngeal chondrosarcomas: a case series and systematic review. *J Neuroimaging*. 2022;32:213-22.
14. Kurokawa R, Baba A, Emile P, et al. Neuroimaging features of angiocentric glioma: a case series and systematic review. *J Neuroimaging*. 2022;32:389-99.
15. Baba A, Kurokawa R, Fukuda T, et al. Comprehensive radiological features of laryngeal sarcoidosis: cases series and systematic review. *Neuroradiology*. 2022;64:1239-48.
16. Kurokawa R, Baba A, Kurokawa M, et al. Neuroimaging of astroblastomas: a case series and systematic review. *J Neuroimaging*. 2022;32:201-12.
17. Kurokawa R, Baba A, Kurokawa M, et al. Neuroimaging features of diffuse hemispheric glioma, H3 G34-mutant: a case series and systematic review. *J Neuroimaging*. 2021;32:17-27.
18. Gojo J, Kjaersgaard M, Zezschwitz BV, et al. Rare embryonal and sarcomatous central nervous system tumours: state-of-the art and future directions. *Eur J Med Genet*. 2022;66:104660.
19. Furuta T, Moritsubo M, Muta H, et al. Central nervous system neuroblastic tumor with FOXR2 activation presenting both neuronal and glial differentiation: a case report. *Brain Tumor Pathol*. 2020;37:100-4.
20. Taschner U, Diebold M, Shah MJ, et al. Freiburg neuropathology case conference: a 6-year-old girl presenting with vomiting and right-sided facial paresis. *Clin Neuroradiol*. 2021;31:885-92.
21. Oztek MA, Noda SM, Romberg EK, et al. Changes to pediatric brain tumors in 2021 World Health Organization classification of tumors of the central nervous system. *Pediatr Radiol*. 2022. <https://doi.org/10.1007/s00247-022-05546-w>
22. Tietze A, Mankad K, Lequin MH, et al. Imaging characteristics of CNS neuroblastoma-FOXR2: a retrospective and multi-institutional description of 25 Cases. *AJNR Am J Neuroradiol*. 2022;43:1476-80.
23. Kurokawa R, Kurokawa M, Baba A, et al. Major changes in 2021 World Health Organization classification of central nervous system tumors. *Radiographics*. 2022;42:1474-93.
24. Łastowska M, Trubicka J, Sobocińska A, et al. Molecular identification of CNS NB-FOXR2, CNS EFT-CIC, CNS HGNET-MN1 and CNS HGNET-BCOR pediatric brain tumors using tumor-specific signature genes. *Acta Neuropathol Commun*. 2020;8:105.
25. Korshunov A, Okonechnikov K, Schmitt-Hoffner F, et al. Molecular analysis of pediatric CNS-PNET revealed nosologic heterogeneity and potent diagnostic markers for CNS neuroblastoma with FOXR2-activation. *Acta Neuropathol Commun*. 2021;9:20.
26. Schmitt-Hoffner F, Van Rijn S, Toprak UH, et al. FOXR2 stabilizes MYCN protein and identifies non-MYCN-amplified neuroblastoma patients with unfavorable outcome. *J Clin Oncol*. 2021;39:3217-28.
27. Poh B, Koso H, Momota H, et al. Foxr2 promotes formation of CNS-embryonal tumors in a Trp53-deficient background. *Neuro Oncol*. 2019;21:993-1004.
28. Liu APY, Dhanda SK, Lin T, et al. Molecular classification and outcome of children with rare CNS embryonal tumors: results from St. Jude Children's Research Hospital including the multi-center SJYC07 and SJMB03 clinical trials. *Acta Neuropathol*. 2022;144:733-46.
29. Dangouloff-Ros V, Varlet P, Levy R, et al. Imaging features of medulloblastoma: conventional imaging, diffusion-weighted imaging, perfusion-weighted imaging, and spectroscopy: from general features to subtypes and characteristics. *Neurochirurgie*. 2021;67:6-13.
30. Kurokawa R, Kurokawa M, Baba A, et al. Dynamic susceptibility contrast-MRI parameters, ADC values, and the T2-FLAIR mismatch sign are useful to differentiate between H3-mutant and H3-wild-type high-grade midline glioma. *Eur Radiol*. 2022;32:3672-82.
31. Arslanoglu A, Aygun N, Tekhtani D, et al. Imaging findings of CNS atypical teratoid/rhabdoid tumors. *AJNR Am J Neuroradiol*. 2004;25:476-80.
32. Tauziède-Espariat A, Debily M-A, Castel D, et al. The pediatric supratentorial MYCN-amplified high-grade gliomas methylation class presents the same radiological, histopathological and molecular features as their pontine counterparts. *Acta Neuropathol Commun*. 2020;8:104.
33. Liu C, Li W, Tong KA, et al. Susceptibility-weighted imaging and quantitative susceptibility mapping in the brain. *J Magn Reson Imaging*. 2015;42:23-41.
34. Mangla R, Kolar B, Zhu T, et al. Percentage signal recovery derived from MR dynamic susceptibility contrast imaging is useful to differentiate common enhancing malignant lesions of the brain. *AJNR Am J Neuroradiol*. 2011;32:1004-10.

**How to cite this article:** Shimazaki K, Kurokawa R, Franson A, Kurokawa M, Baba A, Bou-Maroun L, et al. Neuroimaging features of FOXR2-activated CNS neuroblastoma: A case series and systematic review. *J Neuroimaging*. 2023;33:359–367. <https://doi.org/10.1111/jon.13095>